Journal of Physics: Conference Series **381** (2012) 012006 doi:10.1088/1742-6596/381/1/012006

Precise form factors from elastic electron scattering

J C Bernauer

Massachusetts Institute of Technology, Cambridge, MA 02139-4307, USA

E-mail: bernauer@mit.edu

Abstract. Experiments to determine the electric and magnetic form factors of nucleons have been performed for over half a century. This article gives an overview of the current state of our knowledge and discusses new features discovered in recent high precision experiments.

1. Introduction

The electric and magnetic form factors encode the distribution of charge and magnetization inside the nucleon. Precise determinations of the form factors therefore provide benchmarks for theoretical descriptions, may they be based on effective degrees of freedom or QCD. In the one-photon-exchange approximation, the cross section is given by

$$\left(\frac{\mathrm{d}\sigma}{\mathrm{d}\Omega}\right) = \left(\frac{\mathrm{d}\sigma}{\mathrm{d}\Omega}\right)_{\mathrm{Mott}} \frac{\varepsilon G_E^2 + \tau G_M^2}{\varepsilon\,(1+\tau)}, \tag{1}$$

in terms of the form-factor independent Mott cross section and the two Sachs form factors G_E and G_M.

2. Proton form factors

2.1. Rosenbluth separation

The classical approach to disentangle the form factors from cross section measurements is the Rosenbluth separation [1]. The linear structure of Eq. 1 is exploited to disentangle the form factors at a given Q^2 from several measurements at the chosen Q^2 but with different ε.

The black symbols in Fig. 1 show the progress achieved in the last half century of measurements. After an initial gold rush phase in the 1970s, the focus was on the higher Q^2 range in the 90s. In recent years, with advances in accelerator, detector and experiment design, several experiments achieved a considerable reduction of the uncertainty.

In Fig. 2, both form factors are shown on a logarithmic scale, to demonstrate some of the basic traits: G_E and G_M follow a very similar curve, with a constant factor of μ_p between them, the so-called Scaling relation. In early measurements [2], a dipole was proposed as a simple phenomenological function description:

$$G_E\left(Q^2\right) = 1/\mu_p G_M\left(Q^2\right) = G_{\mathrm{dipole}} = \left(1 + \frac{Q^2}{0.71(\mathrm{GeV}/c)^2}\right)^{-1}. \tag{2}$$

While this simple approximation is still valid as a coarse description, precise measurements show deviations both at low and high Q^2.

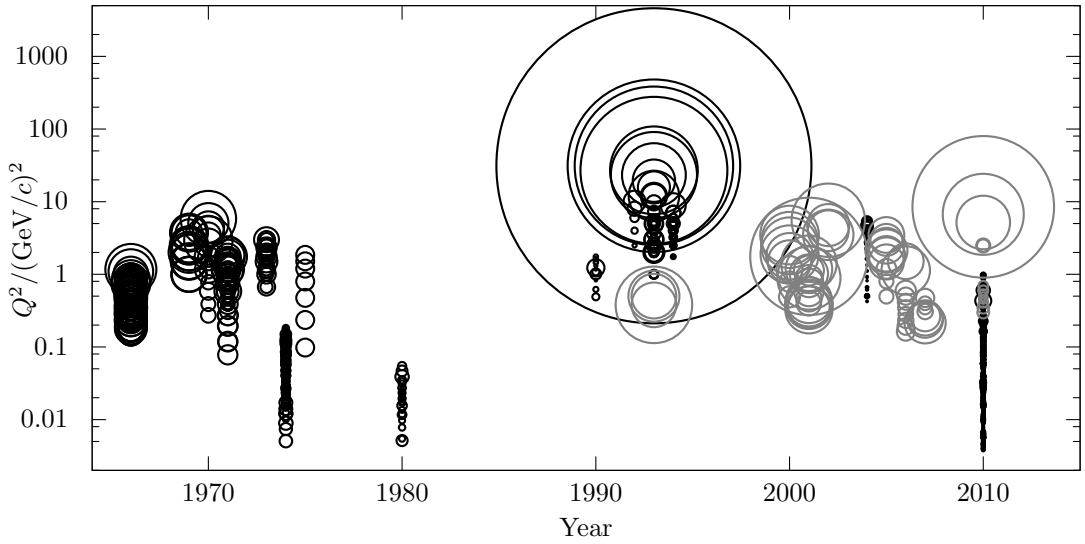

Figure 1. Timeline of proton form factor measurements. The radii of the circles are proportional to the relative uncertainty. Black: unpolarized [3–20], grey: polarized measurements [21–34].

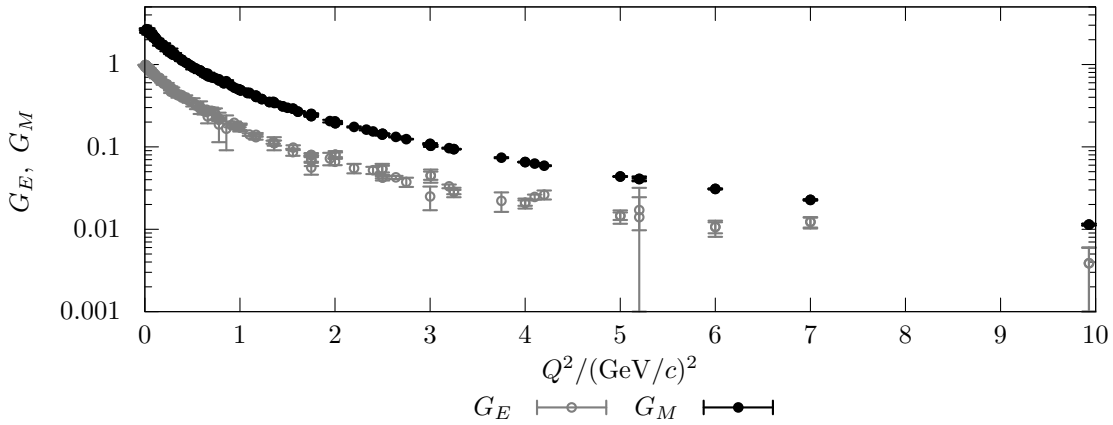

Figure 2. The form factors G_E and G_M extracted from unpolarized measurements.

The figure also exhibits a basic stumble block for the precise determination of G_E for higher Q^2 values. Since G_M is weighted with $\tau \sim Q^2$ in the cross section, the effect of G_E is small in comparison at higher Q^2, and the uncertainty of its determination grows.

2.2. Polarization methods

To reach smaller uncertainties, an alternative approach was developed, based on polarization observables. Two methods are regularly used:

- Polarized electrons are scattered off polarized protons. The double spin asymmetries are then measured.
- With recoil polarimetry, the spin transfer to the recoiling proton is measured when scattering polarized electrons off unpolarized protons.

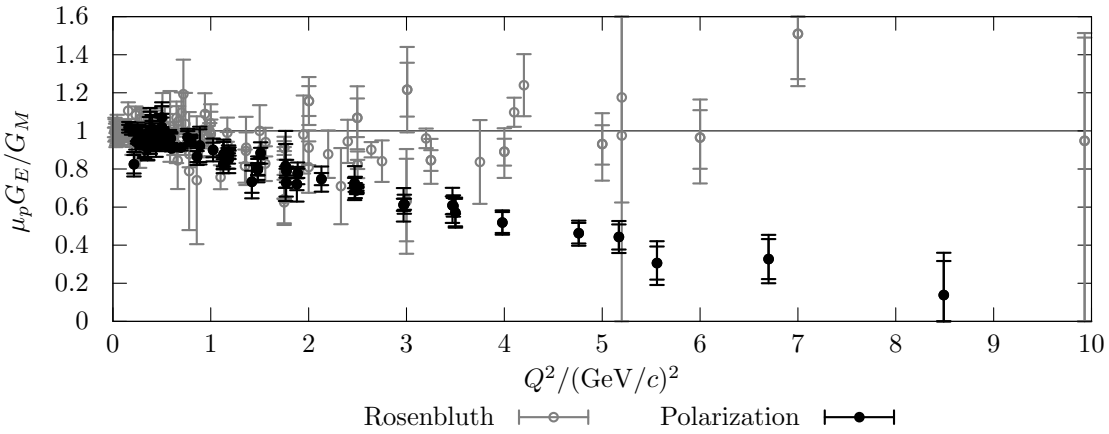

Figure 3. Results for the form factor ratio from unpolarized (grey) and polarized (black) measurements.

Both methods access only the ratio of the form factor, however they do not need an absolute measurement of the cross section. The grey symbols in Fig. 1 illustrate the fast advancements in the use of these comparably new techniques.

2.3. High-Q^2 puzzle

Figure 3 shows the results for the ratio from unpolarized and polarized measurements. While the Rosenbluth data are compatible with the scaling relation prediction, polarized experiments yield data with a linear, downward trend. This discrepancy, which came as a surprise, is understood as a sign of higher-order effects, mainly the two-photon exchange. However, this explanation is not perfect. Theoretical calculations tend to under-predict the effect and only explain about half of the discrepancy. Direct experimental searches for those effects are also puzzling: High precision unpolarized data (e.g., [15]) show that the reduced cross section still is a linear function of ε. The polarization experiment [28] shows an effect only in one polarization variable and yields a zero effect in the form factor ratio, a contradiction to most model calculations.

The underlying theoretical problem is the correct treatment of the intermediate states of the proton between the two-photon exchanges. Vice versa, a precise experimental determination of the effect is a strong test and may hint on how to include these states correctly. The two-photon exchange can be directly measured with the difference between electron-proton and positron-proton scattering, which is the goal of current experiments at DESY, JLab and VEPP-3.

2.4. Low Q^2

The low-Q^2 region was the focus of two recent experiments, one based on the Rosenbluth technique, and one employing polarization observables: The measurement at the Mainz Microtron MAMI [6] encompasses 1422 unpolarized cross section measurements in the Q^2-range up to 1 $(\mathrm{GeV}/c)^2$ (see Fig. 4). In contrast to the usual approach, the form factors and radii were extracted using direct fits of several flexible form factor parametrizations to the cross section data, without the need of an explicit Rosenbluth separation at selected Q^2 values. In these fits, the global normalizations were left floating, using the static limits of the form factors as anchor points. An excellent relative normalization was achieved using one spectrometer to monitor the luminosity.

The extracted magnetic form factor is about 3% larger than previous unpolarized

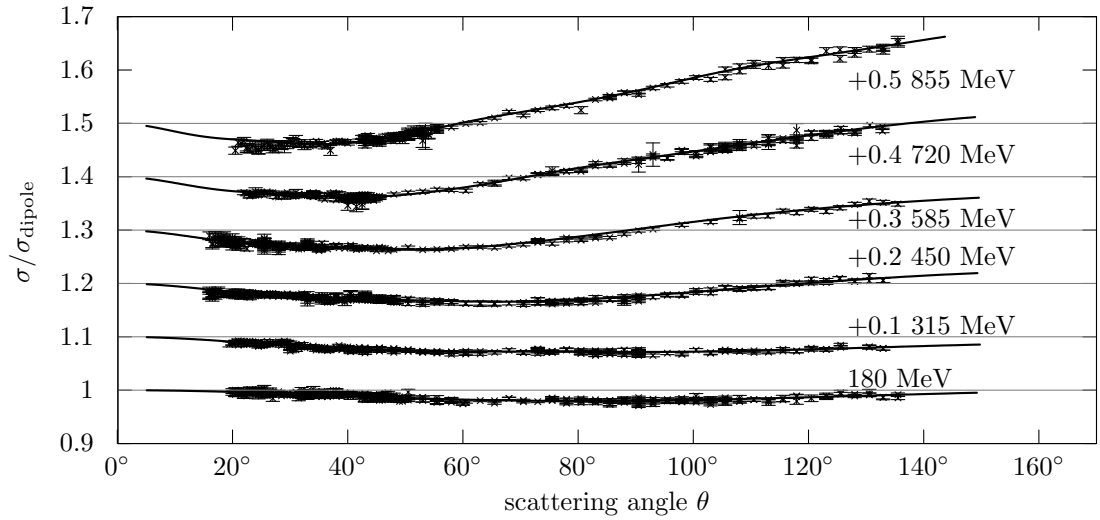

Figure 4. The 1422 cross section measurements of the Mainz experiment [6], divided by the dipole prediction, as a function of the scattering angle. The data points are shifted according to the incident beam energy.

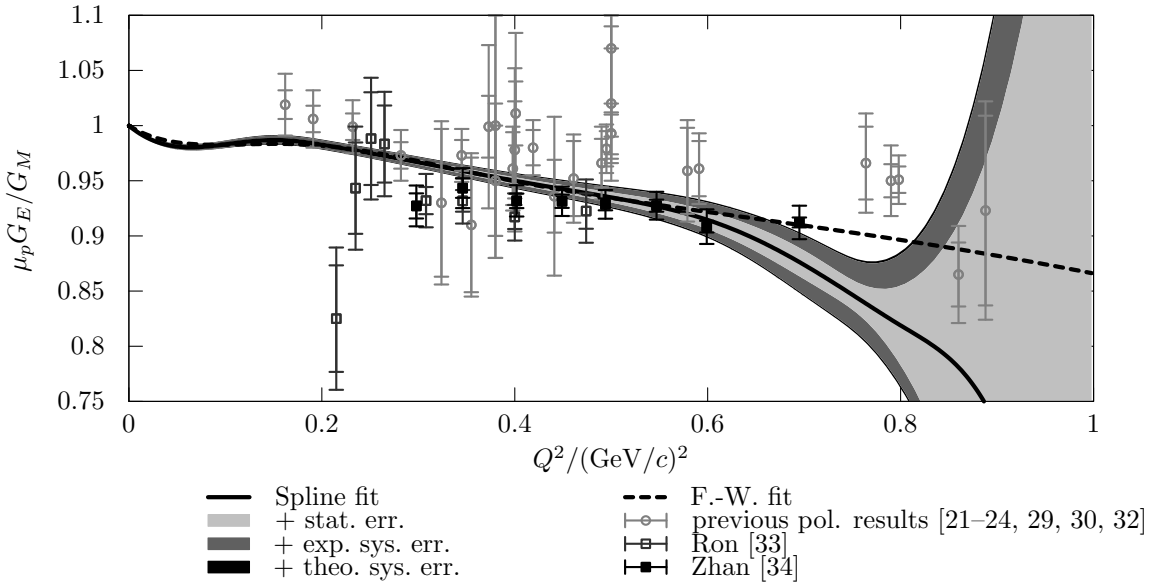

Figure 5. The form factor ratio from polarization experiments and the recent Mainz unpolarized measurement [6]. From the latter, two typical models are shown.

measurements. This, however, brings the form factor ratio into better agreement with the recent polarization experiment [34], where form factor ratios at eight Q^2-values between 0.3 and 0.6 $(\mathrm{GeV}/c)^2$ were extracted. The better understanding of the background situation in this experiment led to a reanalysis of an older experiment [33]. Both experiments show ratios slightly smaller than previous, less precise experiments. In Fig. 5, the results of [6] and [33, 34] are compared to previous polarization results.

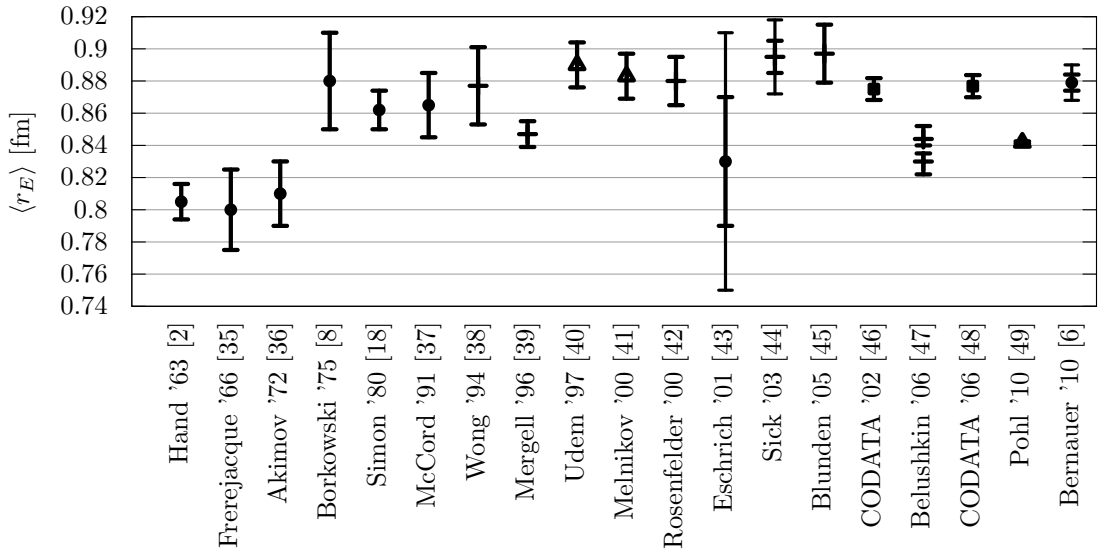

Figure 6. Determinations of the electric proton radius. Circles: electron scattering experiments. Crosses: fits/reanalyses to scattering data, triangles: Hydrogen energy level measurements, rectangles: CODATA fits.

2.5. Proton size puzzle

The proton electric and magnetic radii can be extracted from the slope of the form factors at $Q^2 = 0$. They are also important for corrections to the calculations of atomic energy levels, a focus of QED validity studies. Figure 6 shows the results of the different measurements over the last decades. While there appears to be a number of electron-scattering results, most of the reanalyses are either solely based on or dominated by the Simon et al. [18] data set. However, both electric Hydrogen results and the independent electron-proton scattering result of Bernauer et al. [6] yield compatible values. In contrast to this, Pohl et al. [49], reported a much smaller value, with unpreceded levels of accuracy. They measured level transitions in muonic Hydrogen, where the proton size effect is orders of magnitude larger than in ordinary electric Hydrogen. This $\sim 7\sigma$ difference prompted a large amount of theoretical work, including recalculations of the theoretical corrections, modifications of the form factors at low Q^2 and even physics beyond the standard model. However, no clear explanation has emerged so far.

3. Neutron form factors

The lack of a free neutron target makes determining the neutron form factors much harder, as one has to use deuterium or helium as the target material. For G_E, the measurement is further complicated by the smallness of the form factor itself and by the large ($\sim 50\%$) theoretical corrections.

Figure 7 shows the world data set for the neutron magnetic form factors. The data are again roughly approximated by the dipole up to 4 $(\mathrm{GeV}/c)^2$, at higher Q^2, the data points indicate a strong downward trend. Upcoming data from JLab will cover this region with similar density as the lower Q^2 region.

Due to these experimental challenges, the world data set for the neutron electric form factor is still somewhat limited in size, precision, and Q^2-range, as visible in Fig. 8. Since the electric form factor is so small, almost all measurements employ polarization observables.

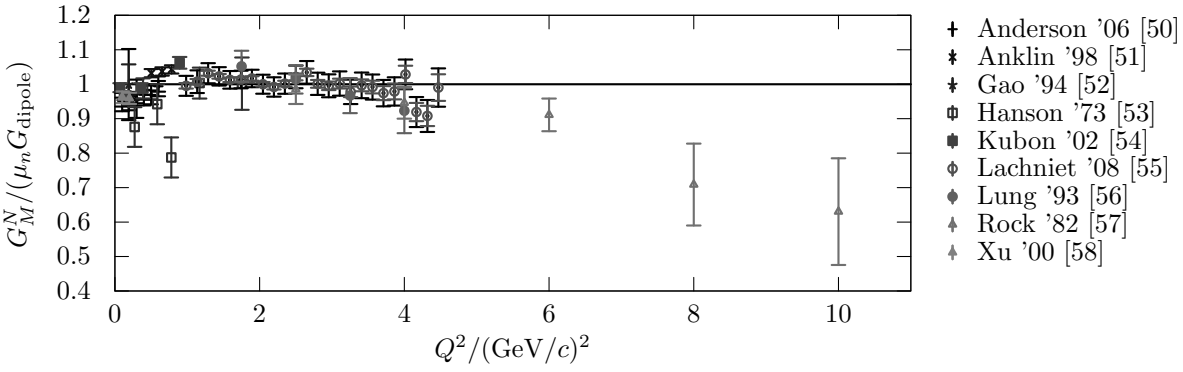

Figure 7. World data set for the neutron magnetic form factor, divided by the dipole prediction.

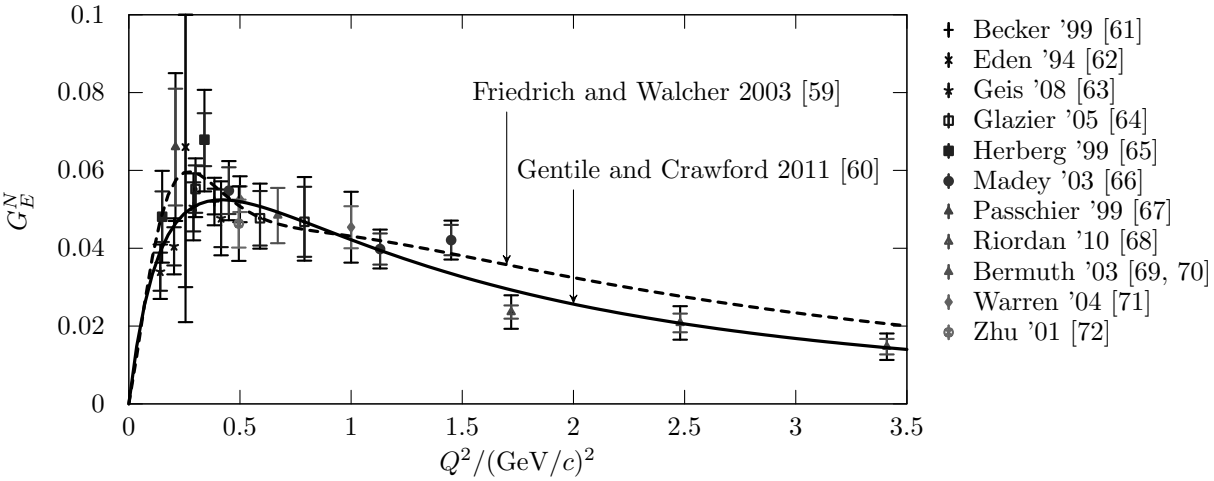

Figure 8. World data set for the neutron electric form factor.

4. Conclusion

In a classical framework, the Fourier transform of the electric and magnetic form factor gives the distribution of charge and magnetization. This has to be modified for a relativistic system, as the transform is only possible in the Breit frame, where the energy transfer to the nucleon vanishes. Figure 9 shows a comparison of the charge distribution according to a dipole form factor and a model [73] composed of the results of [6] for the low-Q^2 and [74] for the high-Q^2 range. Compared to the dipole, charge seems to be pushed out to higher radii, something which would be expected from a pion cloud around the bare proton.

In recent years, a different way of calculating densities has been developed [75]. In the infinite momentum, or light-front frame, one can construct two-dimensional distributions, showing also the difference between a nucleon in a state with defined helicity to one with a polarization perpendicular to the momentum axis.

The precise measurement of the form factors has led to a better understanding of the inner workings of the nucleons. On all scales, the form factor show interesting features which will drive experimentalists and theorists to push both the high-momentum and precision frontier in the upcoming years.

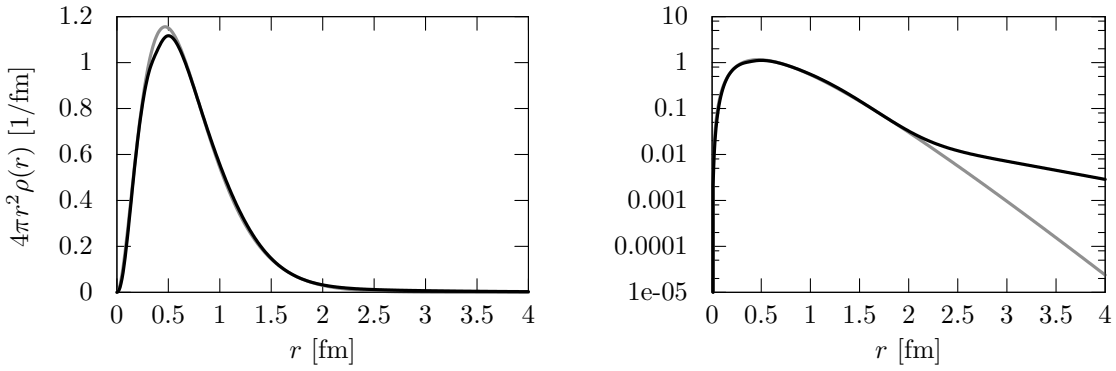

Figure 9. Charge distribution of the proton, calculated from the dipole approximation (grey), and a combined model of low-Q^2 and high-Q^2 fits adapted from [73] (black).

References

[1] Rosenbluth M 1950 *Phys.Rev.* **79** 615–619
[2] Hand L 1963 *Rev.Mod.Phys.* **35** 335
[3] Andivahis L, Bosted P E, Lung A, Stuart L, Alster J *et al.* 1994 *Phys.Rev.* D **50** 5491–5517
[4] Bartel W, Busser F, Dix W, Felst R, Harms D *et al.* 1973 *Nucl.Phys.* B **58** 429–475
[5] Berger C, Burkert V, Knop G, Langenbeck B and Rith K 1971 *Phys.Lett.* B **35** 87
[6] Bernauer J *et al.* (A1 Collaboration) 2010 *Phys.Rev.Lett.* **105** 242001
[7] Borkowski F, Peuser P, Simon G, Walther V and Wendling R 1974 *Nucl.Phys.* A **222** 269–275
[8] Borkowski F, Peuser P, Simon G, Walther V and Wendling R 1975 *Nucl.Phys.* B **93** 461
[9] Bosted P E, Katramatou A, Arnold R, Benton D, Clogher L *et al.* 1990 *Phys.Rev.* C **42** 38–64
[10] Christy M *et al.* (E94110 Collaboration) 2004 *Phys.Rev.* C **70** 015206
[11] Goitein M, Budnitz R, Carroll L, Chen J, Dunning J *et al.* 1970 *Phys.Rev.* D **1** 2449–2476
[12] Janssens T, Hofstadter R, Hughes E and Yearian M 1966 *Phys.Rev.* **142** 922–931
[13] Litt J, Buschhorn G, Coward D, DeStaebler H, Mo L W *et al.* 1970 *Phys.Lett.* B **31** 40–44
[14] Price L, Dunning J, Goitein M, Hanson K, Kirk T *et al.* 1971 *Phys.Rev.* D **4** 45–53
[15] Qattan I, Arrington J, Segel R, Zheng X, Aniol K *et al.* 2005 *Phys.Rev.Lett.* **94** 142301
[16] Rock S, Arnold R, Bosted P E, Chertok B, Mecking B *et al.* 1992 *Phys.Rev.* D **46** 24–44
[17] Sill A, Arnold R, Bosted P E, Chang C, Gomez J *et al.* 1993 *Phys.Rev.* D **48** 29–55
[18] Simon G, Schmitt C, Borkowski F and Walther V 1980 *Nucl.Phys.* A **333** 381–391
[19] Stein S, Atwood W, Bloom E D, Cottrell R, DeStaebler H *et al.* 1975 *Phys.Rev.* D **12** 1884
[20] Walker R, Filippone B, Jourdan J, Milner R, McKeown R *et al.* 1994 *Phys.Rev.* D **49** 5671–5689
[21] Crawford C B, Sindile A, Akdogan T, Alarcon R, Bertozzi W *et al.* 2007 *Phys.Rev.Lett.* **98** 052301
[22] Dieterich S, Bartsch P, Baumann D, Bermuth J, Bohinc K *et al.* 2001 *Phys.Lett.* B **500** 47–52
[23] Gayou O, Wijesooriya K, Afanasev A, Amarian M, Aniol K *et al.* 2001 *Phys.Rev.* C **64** 038202
[24] Gayou O *et al.* (Jefferson Lab Hall A Collaboration) 2002 *Phys.Rev.Lett.* **88** 092301
[25] Jones M *et al.* (Jefferson Lab Hall A Collaboration) 2000 *Phys.Rev.Lett.* **84** 1398–1402
[26] Jones M *et al.* (Resonance Spin Structure Collaboration) 2006 *Phys.Rev.* C **74** 035201
[27] MacLachlan G, Aghalarian A, Ahmidouch A, Anderson B, Asaturian R *et al.* 2006 *Nucl.Phys.* A **764** 261–273
[28] Meziane M *et al.* (GEp2gamma Collaboration) 2011 *Phys.Rev.Lett.* **106** 132501
[29] Milbrath B *et al.* (Bates FPP collaboration) 1998 *Phys.Rev.Lett.* **80** 452–455
[30] Pospischil T *et al.* (A1 Collaboration) 2001 *Eur.Phys.J.* A **12** 125–127
[31] Puckett A, Brash E, Jones M, Luo W, Meziane M *et al.* 2010 *Phys.Rev.Lett.* **104** 242301

[32] Punjabi V, Perdrisat C, Aniol K, Baker F, Berthot J *et al.* 2005 *Phys.Rev.* C **71** 055202
[33] Ron G, Zhan X, Glister J, Lee B, Allada K *et al.* 2011 (*Preprint* `nucl-ex/1103.5784`)
[34] Zhan X 2011 (*Preprint* `nucl-ex/1102.0318`)
[35] Frerejacque D, Benaksas D and Drickey D J 1966 *Phys.Rev.* **141** 1308–1312
[36] Akimov Y, Andert K, Kazarinov Y, Kalinin A, Kiselev V *et al.* 1972 *Sov.Phys.* JETP **35** 651
[37] McCord M, Crannell H, Fagg L, O'Brien J, Sober D *et al.* 1991 *Nucl.Instrum.Meth.* B **56/57** 496–499
[38] Wong C W 1994 *Int.J.Mod.Phys.* E **3** 821–908
[39] Mergell P, Meissner U G and Drechsel D 1996 *Nucl.Phys.* A **596** 367–396
[40] Udem T, Huber A, Gross B, Reichert J, Prevedelli M *et al.* 1997 *Phys.Rev.Lett.* **79** 2646–2649
[41] Melnikov K and van Ritbergen T 2000 *Phys. Rev. Lett.* **84** 1673–1676
[42] Rosenfelder R 2000 *Phys.Lett.* B **479** 381–386
[43] Gough Eschrich I M *et al.* (SELEX Collaboration) 2001 *Phys.Lett.* B **522** 233–239
[44] Sick I 2003 *Phys.Lett.* B **576** 62–67
[45] Blunden P G and Sick I 2005 *Phys.Rev.* C **72** 057601
[46] Mohr P J and Taylor B N 2005 *Rev.Mod.Phys.* **77** 1–107
[47] Belushkin M, Hammer H W and Meissner U G 2007 *Phys.Rev.* C **75** 035202
[48] Mohr P J, Taylor B N and Newell D B 2008 *Rev.Mod.Phys.* **80** 633–730
[49] Pohl R, Antognini A, Nez F, Amaro F D, Biraben F *et al.* 2010 *Nature* **466** 213–216
[50] Anderson B *et al.* (Jefferson Lab E95-001 Collaboration) 2007 *Phys.Rev.* C **75** 034003
[51] Anklin H, deBever L, Blomqvist K, Boeglin W, Bohm R *et al.* 1998 *Phys.Lett.* B **428** 248–253
[52] Gao H, Arrington J, Beise E, Bray B, Carr R *et al.* 1994 *Phys.Rev.* C **50** 546–549
[53] Hanson K, Dunning J, Goitein M, Kirk T, Price L *et al.* 1973 *Phys.Rev.* D **8** 753–778
[54] Kubon G, Anklin H, Bartsch P, Baumann D, Boeglin W *et al.* 2002 *Phys.Lett.* B **524** 26–32
[55] Lachniet J *et al.* (CLAS Collaboration) 2009 *Phys.Rev.Lett.* **102** 192001
[56] Lung A, Stuart L, Bosted P E, Andivahis L, Alster J *et al.* 1993 *Phys.Rev.Lett.* **70** 718–721
[57] Rock S, Arnold R, Bosted P E, Chertok B, Mecking B *et al.* 1982 *Phys.Rev.Lett.* **49** 1139
[58] Xu W, Dutta D, Xiong F, Anderson B, Auberbach L *et al.* 2000 *Phys.Rev.Lett.* **85** 2900–2904
[59] Friedrich J and Walcher T 2003 *Eur.Phys.J.* A **17** 607–623
[60] Gentile T and Crawford C 2011 *Phys.Rev.* C **83** 055203
[61] Becker J, Andresen H, Annand J, Aulenbacher K, Beuchel K *et al.* 1999 *Eur.Phys.J.* A **6** 329–344
[62] Eden T, Madey R, Zhang W, Anderson B, Arenhovel H *et al.* 1994 *Phys.Rev.* C **50** 1749–1753
[63] Geis E *et al.* (BLAST Collaboration) 2008 *Phys.Rev.Lett.* **101** 042501
[64] Glazier D, Seimetz M, Annand J, Arenhovel H, Ases Antelo M *et al.* 2005 *Eur.Phys.J.* A **24** 101–109
[65] Herberg C, Ostrick M, Andresen H, Annand J, Aulenbacher K *et al.* 1999 *Eur.Phys.J.* A **5** 131–135
[66] Madey R *et al.* (E93-038 Collaboration) 2003 *Phys.Rev.Lett.* **91** 122002
[67] Passchier I, Alarcon R, Bauer T, Boersma D, van den Brand J *et al.* 1999 *Phys.Rev.Lett.* **82** 4988–4991
[68] Riordan S, Abrahamyan S, Craver B, Kelleher A, Kolarkar A *et al.* 2010 *Phys.Rev.Lett.* **105** 262302
[69] Rohe D, Bartsch P, Baumann D, Becker J, Bermuth J *et al.* 1999 *Phys.Rev.Lett.* **83** 4257–4260
[70] Bermuth J, Merle P, Carasco C, Baumann D, Bohm D *et al.* 2003 *Phys.Lett.* B **564** 199–204
[71] Warren G *et al.* (Jefferson Lab E93-026 Collaboration) 2004 *Phys.Rev.Lett.* **92** 042301
[72] Zhu H *et al.* (E93026 Collaboration) 2001 *Phys.Rev.Lett.* **87** 081801
[73] Distler M O, Bernauer J C and Walcher T 2011 *Phys.Lett.* B **696** 343–347
[74] Arrington J, Melnitchouk W and Tjon J 2007 *Phys.Rev.* C **76** 035205
[75] Vanderhaeghen M and Walcher T 2010 (*Preprint* `1008.4225`)